Rhodium-Catalyzed Intermolecular Hydroiminoacylation of Alkenes: Comparison of Neutral and Cationic Catalytic Systems

Patricia Marcé,[†] Cyril Godard,*[,‡] Marta Feliz,[§] Xiomara Yáñez,[†,⊥] Carles Bo,*[,‡,§] and Sergio Castillón*[,†]

Departament de Química Analítica i Química Orgànica and Departament de Química Física i Inorgànica, Universitat Rovira i Virgili, C/Marcelí Domingo s/n, 43007 Tarragona, Spain, Institute of Chemical Research of Catalonia (ICIQ), C/Països Catalans 16, 43007 Tarragona, Spain, and Instituto de Investigación en Producción Verde (IPV), Universidad de Pamplona-Sede Villa del Rosario, Cúcuta, Colombia

Received August 25, 2008

Both cationic and neutral rhodium catalytic systems for the hydroiminoacylation of alkenes were studied using NMR spectroscopy and DFT-based methods. With neutral systems, the oxidative addition step was shown to be thermodynamically favored. With the cationic system, the oxidative addition reaction was shown to be endothermic by DFT calculations, and the corresponding intermediate was not detected by NMR. The energy barriers in the cationic and in the neutral pathway are relatively similar. This indicates that the role of chloride when it is coordinated to the rhodium complex is to increase the stability of the oxidative addition product, enabling the reaction to continue. This is not the case in the cationic complexes since the low stability of the reaction products promotes the back reaction, and therefore, low conversions are obtained. The alkene insertion step was also investigated for both systems with styrene as the substrate. The novel neutral complex **21** was detected and fully characterized by multinuclear NMR spectroscopy. In the cationic system, the rhodium hydride styrene intermediate **25** was detected and characterized by NMR spectroscopy. However, no evidence for alkene insertion was found. This study shows that each step of the catalytic cycle is favored in the case of the neutral system when compared with the cationic system.

Introduction

Hydroacylation is an atom-economic, transition-metal-catalyzed process that yields a ketone from an aldehyde and an alkene via C−H bond activation of the aldehyde followed by insertion of the alkene (Scheme 1). The synthetic scope of this reaction is limited by the trend of the metal−acyl intermediates to undergo decarbonylation, affording reduced substrates. This problem can be easily circumvented in the intramolecular version since the coordination of the alkene to give a chelate facilitates the reaction. After the pioneering work by Sakai[1] on intramolecular hydroacylation, mechanistic studies[2] were carried out and this reaction was used for the synthesis of cylopentanones[3] and carbocycles of different sizes.[4] An enantioselective intramolecular hydroacylation process was also successfully used for the synthesis of enantioenriched cyclopentanones.[5]

The development of the intermolecular process is, however, much more challenging, due to the complexity of avoiding the decarbonylation process. Initially, this was achieved by completing the reaction under high pressures (or concentrations) of alkene and/or carbon monoxide.[6] Most of the work on intermolecular hydroacylation, however, has focused on modifying chelation procedures to stabilize the metal−acyl intermediate.[7,8] Chelation assisted by oxygen,[9,10] sulfur,[11] or nitrogen atoms[7,12] in the aldehyde substrate has been reported. Double chelation

* To whom correspondence should be addressed. Fax: (+34) 977 558446. E-mail: sergio.castillon@urv.cat (S.C.). Fax: (+34) 977 559563. E-mail: cyril.godard@urv.cat (C.G.). Fax: (+34) 977 92 0231. E-mail: cbo@iciq.es (C.B.).

† Departament de Química Analítica i Química Orgànica, Universitat Rovira i Virgili.

‡ Departament de Química Física i Inorgànica, Universitat Rovira i Virgili.

§ Institute of Chemical Research of Catalonia (ICIQ).

⊥ Universidad de Pamplona-Sede Villa del Rosario.

(1) Sakai, K.; Ide, J.; Oda, O.; Nakamura, N. *Tetrahedron Lett.* **1972**, *13*, 1287.

(2) (a) Campbell, R. E.; Miller, R. G. *J. Organomet. Chem.* **1980**, *186*, C-27. (b) Campbell, R. E.; Lochow, C. F.; Vora, K. P.; Miller, R. G. *J. Am. Chem. Soc.* **1980**, *102*, 5824. (c) Milstein, D. J. *J. Chem. Soc., Chem. Commun.* **1982**, 1357. (d) Milsten, D. *Acc. Chem. Res.* **1984**, *17*, 221. (e) Fairlie, D. P.; Bosnich, B. *Organometallics* **1988**, *7*, 946.

(3) (a) Sakai, Y.; Ishiguro, K.; Funakoshi, K.; Ueno, K.; Suemune, H. *Tetrahedron Lett.* **1984**, *25*, 961. (b) Fairlie, D. P.; Bosnich, B. *Organometallics* **1988**, *7*, 936. (c) Funakoshi, K.; Togo, N.; Taura, Y.; Sakai, K. *Chem. Pharm. Bull.* **1989**, *37*, 1776.

(4) (a) Gable, K. P.; Benz, G. A. *Tetrahedron Lett.* **1991**, *32*, 3473. (b) Sato, Y.; Oonishi, Y.; Mori, M. *Angew. Chem., Int. Ed.* **2002**, *41*, 1218. (c) Aloise, A. D.; Layton, M. E.; Shair, M. D. *J. Am. Chem. Soc.* **2000**, *122*, 12610.

(5) James, B. R.; Young, C. G. *J. Chem. Soc., Chem. Commun.* **1983**, 1215. (b) Taura, Y.; Tanaka, M.; Funakoshi, K.; Sakai, K. *Tetrahedron Lett.* **1989**, *30*, 6349. (c) Wu, X. M.; Funakoshi, K.; Sakai, K. *Tetrahedron Lett.* **1991**, *33*, 6331. (d) Barnhart, R. W.; Wang, X.; Noheda, P.; Bergens, S. H.; Whelan, J.; Bosnich, B. *J. Am. Chem. Soc.* **1994**, *116*, 1821. (e) Barnhart, R. W.; McMorran, D. A.; Bosnich, B. *Chem. Commun.* **1997**, 589. (f) Tanaka, K.; Fu, G. *J. Am. Chem. Soc.* **2001**, *123*, 11492. (g) Tanaka, K.; Fu, G. *J. Am. Chem. Soc.* **2002**, *123*, 10296. (h) Kundu, K.; McCullagh, J. V.; Morehead, A. T., Jr. *J. Am. Chem. Soc.* **2005**, *127*, 16042.

(6) (a) Marder, T. B.; Roe, D. C.; Milstein, D. *Organometallics* **1988**, *7*, 1451.

(7) Suggs, J. W. *J. Am. Chem. Soc.* **1978**, *100*, 640.

(8) For a recent review, see: Jun, C.-H.; Jo, E.-A.; Park, J.-W. *Eur. J. Org. Chem.* **2007**, 1869.

(9) (a) Kokubo, K.; Matsumasa, K.; Nishinaka, Y.; Miura, M.; Nomura, M. *Bull. Chem. Soc. Jpn.* **1999**, *72*, 303. (b) Miura, M.; Nomura, M. *J. Synth. Org. Chem. Jpn.* **2000**, *58*, 578.

(10) The first asymmetric version of the intermolecular hydroacylation of norbornenes with *o*-hydroxybenzaldehyde has been recently reported: Stemmler, R. T.; Bolm, C. *Adv. Synth. Catal.* **2007**, *349*, 1185.

10.1021/om800827r CCC: $40.75
Publication on Web 04/22/2009

Scheme 1. Intermolecular Hydroacylation Reaction

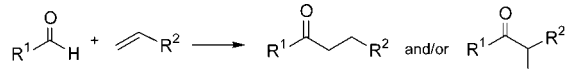

methods, in which both the aldehyde and the alkene coordinate to the rhodium center in a bidentate manner, and alkene chelation involving an amide group have also been successfully developed.[13] The use of anhydrides as acylating reagents[14] or [RhCp*][15] catalysts does not require chelation assistance.

Suggs showed that 2-amino-picoline-derived aldimines react with alkenes in the presence of $[RhCl(PPh_3)_3]$ to give ketimines.[16] Jung developed a one-pot intermolecular hydroacylation procedure that forms in situ the 2-amino-picoline aldimine derivative, which reacts with an alkene in the presence of Wilkinson's catalyst to yield a ketimine.[17] Later, the ketimine is hydrolyzed within the reaction media to provide the ketone (Scheme 2). This procedure avoids the use of a coordinating atom that is permanently bound to the substrate. This method was also successfully applied in the hydroacylation of alkynes.[18]

The mechanism of the intramolecular hydroacylation reaction has already been studied using both neutral[2,19] and cationic precursors.[2e] The rate-limiting step of this reaction is the reductive elimination of the product. Recently, a detailed computational study provided additional insights into this mechanism.[20] In contrast, the mechanism of intermolecular hydroacylation has been much less studied but is thought to be similar to that of the intramolecular version.[6−13] When the reaction was studied using deuterated benzaldehyde and ethene pressure, deuterium in the organic product was found in the methyl and methylene groups in a ratio of 3:2, indicating that the alkene insertion was a reversible process.[6] In another study, reductive elimination was proposed to be the rate-determining step, with other steps of the catalytic cycle described as reversible processes.[2e,21]

The mechanism of the one-pot 2-picoline-assisted intermolecular hydroacylation procedure has not yet been investigated. The catalytic cycle proposed for this reaction involves the following classical steps: the oxidative addition of the aldimine, followed by the coordination and insertion of the alkene into the Rh−H bond of the catalyst, and the reductive elimination of the product and the regeneration of the starting Rh species.[22]

In the context of the work carried out in our laboratory on the Rh-catalyzed hydroiminoacylation of alkenes, the catalytic results revealed a strong difference between the activity of neutral and cationic catalysts in the one-pot 2-picoline-assisted intermolecular hydroacylation. Here, we report these catalytic results and a comparative mechanistic study of the intermolecular hydroiminoacylation of alkenes with the aldimine **3** between neutral and cationic rhodium systems using in situ NMR techniques and computational DFT-based methods.

Results and Discussion

Catalysis. In the course of a study of the one-pot 2-picoline-assisted intramolecular hydroacylation of alkenes[23] and alkynes,[24] the use of Montmorillonite K-10 (MK-10) as a reusable acid catalyst able to catalyze the imine formation and ketimine hydrolysis (see first and last steps in Scheme 2), was previously explored. Furthermore, MK-10 can also be used as a solid support for immobilizing and recovering the catalyst, and for this purpose, cationic complexes are required.[25] We therefore studied a series of cationic precursors of the formula $[Rh(cod)(L)_2]BF_4$, where L corresponds to phosphine and phosphite ligands, in the presence of 2-amino-3-picoline and MK-10 (Table 1). The hydroacylation reaction described should be considered as a sequence of three successive reactions: the formation of aldimine **3**, the Rh-catalyzed hydroiminoacylation leading to ketimine **9**, and the hydrolysis of **9** yielding **10**. The rhodium catalyst is thus only involved in the hydroiminoacylation reaction, while MK-10 catalyzes the two other processes.

Comparing the results shown in entries 1−6, it is apparent that the neutral system $[RhCl(PPh_3)_3]$ (entry 1) provides a much higher conversion than any of the cationic catalytic systems (entries 2−6). Low conversions were obtained when monophosphines with different electronic properties (entries 2−5) were used. When a monophosphite ligand (entry 6) was used, no conversion was observed. However, when a source of chloride was added to the reaction mixture (entry 7), a comparable conversion to that obtained with the neutral system was achieved (75%). This result suggested that, under these conditions, the neutral rhodium catalytic system was restored.

Identical result was obtained when the reaction was performed starting from aldimine **3**, indicating that the nature of the rhodium catalyst was the key to explain the behavior of these catalytic systems.

In light of these results, a mechanistic study using in situ NMR and DFT calculations was undertaken in order to gain insight into the difference of behavior between the neutral and the cationic rhodium systems catalyzing the 2-picoline-assisted intramolecular hydroacylation of alkenes.

Study of the Oxidative Addition by in situ NMR. Neutral System. Initially, this process was investigated by NMR spectroscopy. A THF-d_8 solution of $RhCl(PPh_3)_3$ was charged

(11) (a) Willis, M. C.; Randell-Sly, H. E.; Woodward, R. L.; McNally, S. J.; Currie, G. S. *J. Org. Chem.* **2006**, *71*, 5291. (b) Moxham, G. L.; Randell-Sly, H. E.; Brayshaw, S. K.; Woodward, R. L.; Weller, A. S.; Willis, M. C. *Angew. Chem., Int. Ed.* **2006**, *45*, 7618. (c) Willis, M. C.; Randell-Sly, H. E.; Woodward, R. L.; Currie, G. S. *Org. Lett.* **2005**, *7*, 2249. (d) Willis, M. C.; McNally, S. J.; Beswick, C. J. *Angew. Chem., Int. Ed.* **2004**, *43*, 340.

(12) Wojcicki, A. *Adv. Organomet. Chem.* **1973**, *11*, 87.

(13) Imai, M.; Tanaka, M.; Tanaka, K.; Yamamoto, Y.; Ogata-Imai, N.; Shimowatari, M.; Nagumo, S.; Kawahara, N.; Suemune, H. *J. Org. Chem.* **2004**, *69*, 1144. (b) Tanaka, M.; Imai, M.; Yamamoto, Y.; Tanaka, K.; Shimowatari, M.; Nagumo, S.; Kawahara, N.; Suemune, H. *Org. Lett.* **2003**, *5*, 1365. (c) Tanaka, K.; Tanaka, M.; Suemune, H. *Tetrahedron Lett.* **2005**, *46*, 6053.

(14) Hong, T.-K.; Barchuck, A.; Krische, M. J. *Angew. Chem., Int. Ed.* **2006**, *45*, 6885.

(15) Roy, A. H.; Lenges, C. P.; Brookhart, M. *J. Am. Chem. Soc.* **2007**, *129*, 2082.

(16) Suggs, J. W. *J. Am. Chem. Soc.* **1979**, *101*, 489.

(17) (a) Park, Y.-J.; Park, J.-W.; Jun, C.-H. *Acc. Chem. Res.* **2008**, *41*, 222. (b) Jun, C.-H.; Moon, C. W.; Lee, D. Y. *Chem.—Eur. J.* **2002**, *8*, 2423. (c) Jun, C.-H.; Lee, D. Y.; Lee, H.; Hong, J.-B. *Angew. Chem., Int. Ed.* **2000**, *39*, 3070. (d) Jun, C.-H.; Hong, J.-B. *Org. Lett.* **1999**, *1*, 2161.

(18) (a) Jun, C.-H.; Lee, H.; Hong, J.-B.; Kwon, B. I. *Angew. Chem., Int. Ed.* **2002**, *41*, 2146. (b) Lee, D. Y.; Hong, B. S.; Cho, E. G.; Lee, H.; Jung, C.-H. *J. Am. Chem. Soc.* **2003**, *125*, 6372. (c) Jun, C.-H.; Lee, H. *Pure Appl. Chem.* **2004**, *76*, 577.

(19) Lau, K. Y.; Becker, Y.; Huang, F.; Baenziger, N.; Stille, J. K. *J. Am. Chem. Soc.* **1977**, *99*, 566.

(20) Hyatt, I. E. D.; Anderson, H. K.; Morehead, A. T.; Sargent, A. L. *Organometallics* **2008**, *17*, 135.

(21) (a) Bosnich, B. *Acc. Chem. Res.* **1998**, *31*, 667. (b) Barnhart, R. W.; Bosnich, B. *Organometallics* **1995**, *14*, 4343.

(22) (a) Jun, C.-H.; Lee, H. *J. Am. Chem. Soc.* **1999**, *121*, 880. (b) Jun, C.-H.; Lee, H.; Hong, J.-B. *J. Org. Chem.* **1997**, *62*, 1200. (c) Jun, C.-H.; Hoh, C.-W.; Na, S.-J. *Angew. Chem., Int. Ed.* **1998**, *37*, 145. (d) Jun, C.-H. *Chem. Soc. Rev.* **2004**, *33*, 610.

(23) Yáñez, X.; Claver, C.; Castillón, S.; Fernández, E. *Tetrahedron Lett.* **2003**, *44*, 1631.

(24) Yáñez, X.; Castillón, S. *J. Organomet. Chem.* **2007**, *692*, 1628.

(25) Claver, C.; Fernández, E.; Margalef-Català, R.; Medina, P.; Salagre, P.; Sueiras, J. P. *J. Catal.* **2001**, *201*, 70.

Scheme 2. Proposed Mechanism for the 2-Picoline-Assisted Intermolecular Hydroacylation of Alkenes

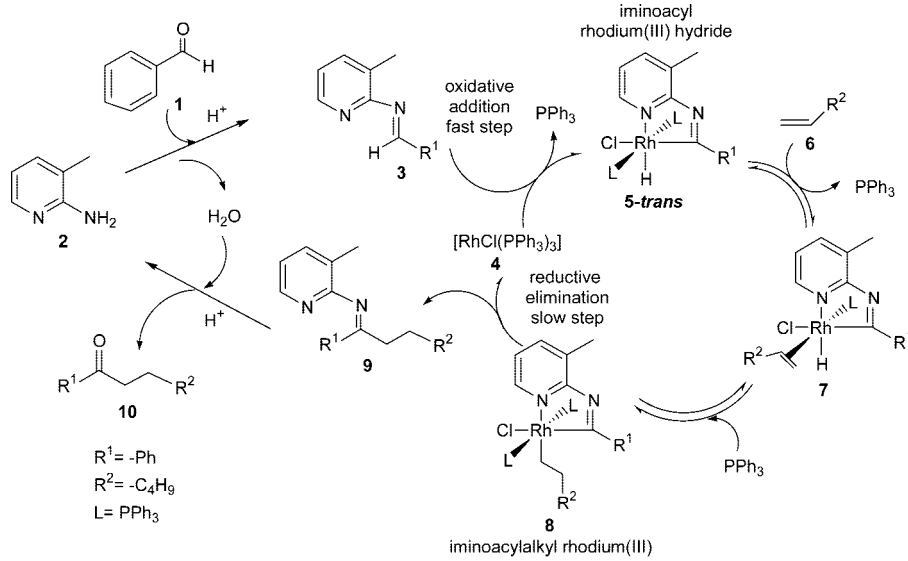

Table 1. Hydroiminoacylation Reaction of Aldimine 3, Formed in situ from Benzaldehyde (1), with 1-Hexene in the Presence of $RhClL_3$ and $[Rh(cod)L_2]BF_4$[a]

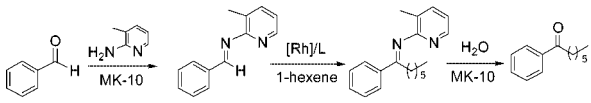

1 3 9 10

entry	[Rh]	ligand (L)	conv (%)[b]
1	$[RhCl(PPh_3)_3]$		80[c]
2	$[Rh(cod)L_2]BF_4$	PPh_3	7
3	$[Rh(cod)L_2]BF_4$	$(p\text{-Me-Ph})_3P$	11
4	$[Rh(cod)L_2]BF_4$	$(p\text{-F-Ph})_3P$	7
5	$[Rh(cod)L_2]BF_4$	Ph_2EtP	9
6	$[Rh(cod)L_2]BF_4$	$(MeO)_3P$	0
7[d]	$[Rh(cod)L_2]BF_4$	$(p\text{-Me-Ph})_3P$	75[e]

[a] Conditions: benzaldehyde (2.5 mmol), hexene (12.5 mmol), 2-amino-3-picoline (0.8 mmol), $[Rh(cod)L_2]BF_4$ (0.05 mmol), free ligand added (0.05 mmol), MK-10 (80 mg), toluene (2 mL), 110 °C, 2 h. [b] Conversion of the rhodium-catalyzed reaction expressed as the ratio of **9** + **10** to **1** + **3** measured by GC (chromatograph Hewlett-Packard 5890A, HP-5 column, T = 80 °C for 0.5 min up to 280 °C; rate = 10 °C/min). [c] Ratio in %: **1/3/9/10** = 18:2:10:70. [d] $BnMe_3NCl$ (0.05 mmol) was added. [e] Ratio in %: **1/3/9/10** = 22:3:15:60.

Scheme 3. Reactivity of $RhCl(PPh_3)_3$ in the Presence of Aldimine 3 in THF

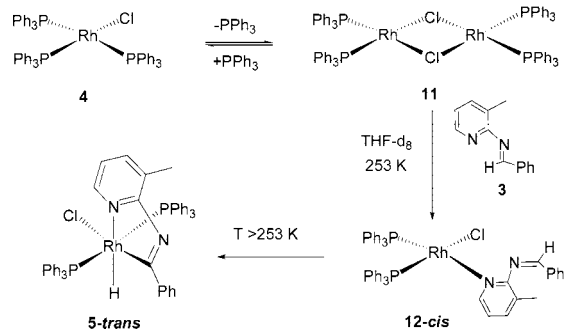

into a 5 mm NMR tube fitted with a Young's tap. In the corresponding $^{31}P\{^1H\}$ spectrum, signals arising from this complex, the rhodium dimer $[Rh(\mu\text{-Cl})(PPh_3)_2]_2$ (**11**), and free PPh_3 were readily detected (Scheme 3). One equivalent of aldimine **3** was then added at room temperature under inert atmosphere, and a new $^{31}P\{^1H\}$ spectrum was acquired. At this point, a new doublet signal at δ 33.1 (J_{RhP} = 116.6 Hz) was detected as the main species (90%) in solution, and the signal arising from PPh_3 increased in intensity. In the ^1H spectrum a hydride signal was observed at δ −11.14 (q, $J_{RhH} = J_{PH}$ = 13 Hz) and readily assigned to the oxidative addition product ***5-trans***.[16,26] It was therefore concluded that, at this temperature, the oxidative addition reaction occurs very rapidly.

When the reaction was repeated at low temperature, no new signals were detected between 193 and 243 K by ^1H and ^{31}P NMR spectroscopy. However, when the temperature of the sample was increased to 253 K, the signal corresponding to $[Rh(\mu\text{-Cl})(PPh_3)_2]_2$ initially detected in the $^{31}P\{^1H\}$ spectrum was found to be lower in intensity, and two new doublet of doublets at δ 54 and 50 (J_{RhP} = 196 and 170 Hz, J_{PP} = 47 Hz) appeared, which were assigned to two inequivalent phosphine ligands of a new species. In the corresponding ^1H spectrum, new low field signals were detected at δ 9.1 (s) and 9.0 (dd, J_{HH} = 1.8 and 5 Hz). A COSY experiment showed that the signal at δ 9.0 was correlated to two proton resonances in the aromatic region at δ 7.2 and 6.85, which were assigned to the pyridyl unit of a new aldimine ligand. The chemical shift of the resonance at δ 9.0 indicated that the pyridyl unit was coordinated to a Rh center through the N atom. The signal at δ 9.1 was assigned to the N=CHPh group based on its similarity with the signal corresponding to free aldimine. The new compound formed was therefore identified as *cis*-$[RhCl(PPh_3)_2(3)]$ (***12-cis***, Scheme 3). Very similar NMR features were reported for the analogue complex $[RhCl(PPh_3)_2(pyridine)]$.[26,27a,b]

At this stage, the temperature of the sample was increased to 258 K. In the $^{31}P\{^1H\}$ spectrum, the signal corresponding to $[Rh(\mu\text{-Cl})(PPh_3)_2]_2$ was not detected; the resonances for ***12-cis*** were found to increase in intensity, and the signal corresponding to the oxidative addition product ***5-trans*** was detected at δ 32.6 (J_{RhP} = 116 Hz) and slowly increased in intensity.

The detection and NMR characterization of species *cis*-$[RhCl(PPh_3)_2(3)]$ (***12-cis***) indicated that the oxidative addition

(26) Albinati, A.; Arz, C.; Pregosin, P. S. *J. Organomet. Chem.* **1987**, *335*, 379.

(27) (a) Heaton, B. T.; Iggo, J. A.; Jacob, C.; Nadarajah, J.; Fontaine, M. A.; Messere, R.; Noels, A. F. *J. Chem. Soc., Dalton Trans.* **1994**, 2875. (b) Retondo, E.; Battaglia, G.; Arena, C. G.; Faraone, F. *J. Organomet. Chem.* **1991**, *419*, 399. (c) Elsevier, C. J.; Kowall, B.; Kragten, H. *Inorg. Chem.* **1995**, *34*, 4836. (d) Carlton, L.; De Sousa, G. *Polyhedron* **1993**, *12*, 1377.

Scheme 4. Reactivity of Cationic Complex 13 in the Presence of Aldimine 3 and $BnMe_3NCl$

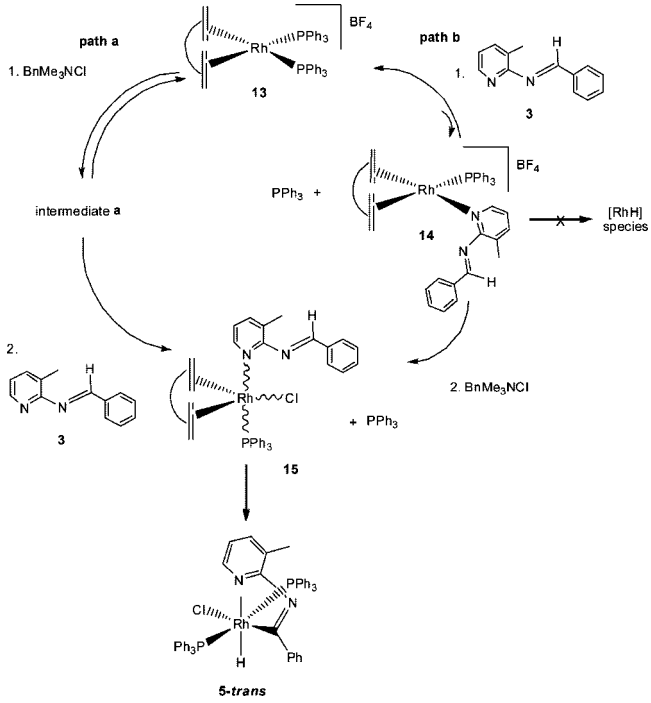

step was initiated by the coordination of the aldimine **3** through the nitrogen atom of the pyridyl unit (Scheme 3), and that this process takes place at temperatures higher than 253 K (Scheme 3).

Cationic System. Reaction of $[Rh(NBD)(PPh_3)_2]BF_4$ (13) in the Presence of Aldimine 3. In order to study the oxidative addition process using the cationic system, the reactivity of the cationic precursor $[Rh(NBD)(PPh_3)_2]BF_4$ (**13**) in the presence of aldimine **3** was first investigated (Scheme 4). A THF-d_8 solution containing the complex **13** was charged into an NMR tube, and ^1H and $^{31}P\{^1H\}$ NMR spectra were recorded at room temperature. The expected signals for **13** were readily detected (Table 2). Two equivalents of aldimine **3** was then added under inert atmosphere, and a ^1H spectrum was immediately recorded at room temperature. The signals corresponding to **3** were readily detected as sharp signals. The resonances corresponding to the NBD ligand of **13**, however, were this time observed as broad signals. In the $^{31}P\{^1H\}$ spectrum, the signal at δ 31.6 was observed as a very broad resonance, and no Rh−P coupling constant could be measured. At 333 K, two very broad signals were detected at δ −1.5 and 30.2 in the $^{31}P\{^1H\}$ spectrum. These resonances were assigned to free PPh_3 and **13**, respectively (Scheme 4). Although the resonances of PPh_3 and **13** are usually observed at ca. δ −5 and 31.6, respectively, a fast equilibrium between these species could explain such a shift. The detection of free PPh_3 suggests that substitution of a PPh_3 by **3** had occurred, affording $[Rh(NBD)(PPh_3)(\mathbf{3})]BF_4$ (**14**) (Scheme 4, path b1). It can be concluded that a fast equilibrium between **13** and **14** was taking place. However, it is noteworthy that during this study no hydride signal was detected, even when the solution was heated, which indicates that no stable oxidative addition product ([RhH] species) was formed under these conditions.

Reaction of $[Rh(NBD)(PPh_3)_2]BF_4$ (13) in the Presence of the Aldimine 3 and $BnMe_3NCl$. As shown in Table 1, cationic rhodium complexes were scarcely active or inactive in the intermolecular hydroacylation (entries 2−6). However, the activity was restored when a chloride source was added (entry 9). In order to investigate the role of chlorine, the sample used in the previous study containing $[Rh(NBD)(PPh_3)_2]BF_4$ (**13**) and aldimine **3** was cooled to room temperature, and 3 equiv of $BnMe_3NCl$ was added under inert atmosphere (Scheme 4, path b2). When a ^1H spectrum was recorded, the signals corresponding to the NBD ligand of **13** were not observed, and three new signals at δ 4.10, 3.69, and 3.11 were detected and assigned to an NBD ligand of a new species formed under these conditions. In the aromatic region, due to the overlapping of signals arising from PPh_3 ligands, the aldimine **3**, and $BnMe_3NCl$, no clear changes could be observed. In the corresponding $^{31}P\{^1H\}$ spectrum, a new broad resonance at δ 16.7 was observed as the only signal. In order to reduce the high fluxionality of this species, low temperature spectra were recorded. However, at 193 K, the signal was still very broad. It was therefore concluded that a new Rh complex containing at least one chelating NBD and one PPh_3 ligand was formed. Structure **15** was proposed for this complex. Given the high fluxionality of the complex formed and the large shifts observed in ^{31}P NMR, we concluded that the signal detected at δ 16.7 arose from an average of the signals corresponding to the coordinated PPh_3 ligand from **15** and the free ligand. Indeed, the reported chemical shifts for complexes containing PPh_3, alkenes, chloride, and a nitrogen donor usually lie above 30 ppm, and although such signals were not detected, shifts toward this region were always observed when the temperature was lowered and the ligand exchange rate was thereby reduced.[27c,d]

Compound **15** was also formed when the order of addition of reagents was reversed by adding first $BnMe_3NCl$ and second the aldimine **3** (Scheme 4, path a1). In this case, the ^1H NMR spectrum of a THF-d_8 solution of **13** and 3 equiv of $BnMe_3NCl$ showed three new NBD signals at δ 4.32, 3.87, and 2.52, indicating the formation of a new intermediate **a**. Surprisingly, in the corresponding $^{31}P\{^1H\}$ spectrum, no signals could be detected. This observation indicated that a highly fluxional process was occurring under these conditions.

Indeed, when the temperature of the sample was decreased to 233 K, a new broad signal was observed at δ 20.8. However, due to the high fluxionality of this species, even at lower temperatures, their identity could not be determined unambiguously. Such a behavior was previously reported for Rh cationic systems containing a weakly coordinated halide ligand.[28] After the addition of 2 equiv of aldimine **3** to the solution, only the signal at δ 16.7 corresponding to the species **15** was detected in the $^{31}P\{^1H\}$ spectrum (Scheme 4, path a2).

When the samples containing **15** were warmed to 343 K, on the ^1H NMR and $^{31}P\{^1H\}$ spectrum, a hydride signal at δ −11.14 (q, $J_{RhH} = J_{PH} =$ 13 Hz) and a doublet signal δ 33.1 ($J_{RhP} =$ 116 Hz), respectively, corresponding to ***5-trans*** were detected. After several hours at 343 K, total conversion to ***5-trans*** was achieved. The detection of ***5-trans*** indicated that the oxidative addition process had occurred in the presence of chloride and that it was now coordinated to the rhodium center (Scheme 4).

The results described in this section demonstrate that the cationic rhodium complex $[Rh(NBD)(PPh_3)_2]BF_4$ (**13**) does not react with aldimine **3** to give any stable oxidative addition products. However, in the presence of $BnMe_3NCl$, the hydride species ***5-trans*** formed by oxidative addition of **3** is readily

(28) (a) Delis, J. G. P.; Aubel, P. G.; Vrieze, K.; van Leeuwen, P. W. N. M. *Organometallics* **1997**, *16*, 2948. (b) Groen, J. H.; van Leeuwen, P. W. N. M.; Vrieze, K. *J. Chem. Soc., Dalton Trans.* **1998**, 113. (c) Romeo, R.; Fenech, L.; Scolaro, L. M.; Albinati, A.; Macchioni, A.; Zuccaccia, C. *Inorg. Chem.* **2001**, *40*, 3293. (d) Albinati, A.; Kunz, R. W.; Amman, C. J.; Pregosin, P. S. *Organometallics* **1991**, *19*, 1800. (e) Gogoll, A.; Ornebro, J.; Grennberg, H.; Backwall, J. E. *J. Am. Chem. Soc.* **1994**, *116*, 3631.

Table 2. Selected NMR Data for the Complexes 5-*trans*, 13, and 14

		^{1}H NMR			^{31}P NMR	
complex	T (K)	ligand	δ in ppm[a]	ligand	δ in ppm	J_{RhP}
5-trans	rt	hydride	−11.14 (dt)	PPh_3	33.1 (br s)	116.6
13	rt	NBD	2.51 (s, 2H), 4.12 (s, 2H), 4.64 (s, 4H)	PPh_3	31.6 (br s)	156
15	rt	NBD	3.11 (s, 2H), 3.69 (s, 2H), 4.10 (s, 4H)	PPh_3	16.7 (brs)[b]	

[a] The ^{1}H NMR spectra were recorded at room temperature. [b] This signal has been proposed to arise from the average of **15** and free PPh_3, which are in equilibrium.

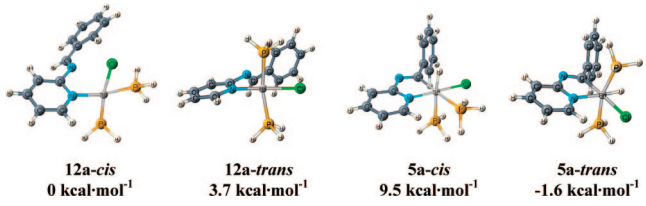

Figure 1. Molecular structures and relative energies for isomers *cis* and *trans* of the species **12a** and **5a**.

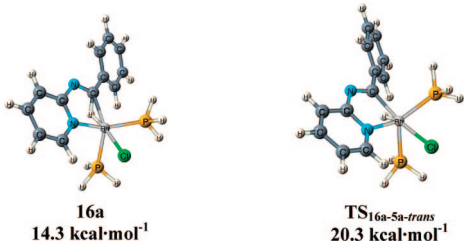

Figure 2. Molecular structures and relative energies, referred to as **12a-*trans***, for the species involved in the reaction coordinate of the neutral complex.

detected as the only organometallic product. This reaction was shown to occur via the formation of the Rh phosphine complex **15** (Scheme 4).

Study of the Oxidative Addition by DFT Calculations. The oxidative addition step of the intermolecular hydroiminoacylation was examined in both neutral and cationic systems. Intermediates and the corresponding transition states were determined for the neutral precursor [Rh(aldimine)$(PH_3)_2$Cl] (**12a**). Although **14** (Scheme 4) is the only intermediate detected by NMR from the cationic complex **13** in the presence of aldimine **3** (Scheme 4, path b), it is reasonable to consider that this species must lose NBD and that aldimine or phosphine must coordinate to rhodium before the oxidative addition takes place. Accordingly, we considered two possible structures: complex [Rh(aldimine)$(PH_3)_2]^+$ (**17a**), where aldimine is coordinated in a chelate manner (Figure 3), and complex [Rh(aldimine)$_2(PH_3)_2]^+$, where aldimine is coordinated only through the pyridinic nitrogen. For simplifying the computational cost, one aldimine has been substituted by pyridine, complex [Rh(aldimine)(py)$(PH_3)_2]^+$ (**21a**) (Figure 4).

For the neutral system, complex **12a** and the corresponding oxidative addition product **5a** were considered, in both their *cis* and the *trans* isomers (Figure 1). These results indicated that **12a-*cis***, in which the two phosphine ligands are located in a *cis* fashion, corresponds to the most stable isomer, which is precisely the species **12-*cis*** characterized by NMR experiments. However, the most stable product of the oxidative addition process is **5a-*trans***, and therefore, the reaction from **12a-*cis*** to **5a-*trans*** is exothermic by 1.6 kcal·mol^{-1} (Figure 1). This result is also in full agreement with the NMR experiments described earlier (see Supporting Information for a comparison between X-ray data of the **5-*trans*** iodide complex described by Albinati et al.[26] and our computed DFT geometry). The oxidative

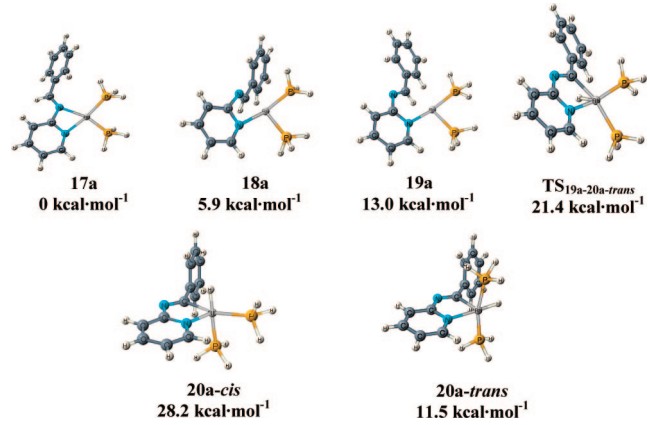

Figure 3. Molecular structures and relative energies for **17a**, *cis* and *trans* isomers for **20a**, intermediates **18a** and **19a**, and the corresponding transition state.

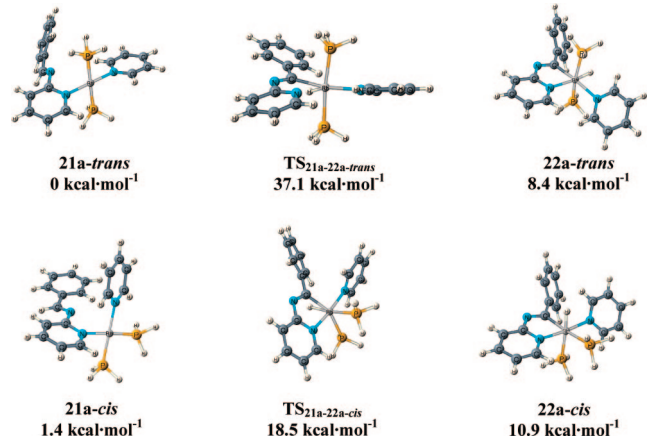

Figure 4. Molecular structures and relative energies for species involved in the reaction of the cationic complex with an additional pyridine ligand.

addition process for species **12a-*cis*** to **5a-*trans*** was therefore studied. During the transition state search, a new intermediate was characterized (**16a**, Figure 2) that shows an interaction between the rhodium center and the C−H bond involved in the oxidative addition process. Note that in this structure the angle between the two phosphine ligands increased (101.5°) and that the C−H bond is elongated (1.102 Å in free aldimine **3**, 1.412 Å in **16a**). This structure was computed to be above the reactant by 14.3 kcal·mol^{-1}. The corresponding transition state (**TS$_{16a\text{-}5a\text{-}trans}$**) was fully characterized and is shown in Figure 2. Here, we noted a close resemblance to the agostic intermediate, especially in regard to the P−Rh−P angle of 117.6° and the C−H bond length (1.759 Å). The energy difference between the transition state and the agostic intermediate is small, only 6.0 kcal·mol^{-1}, indicating the reactant-like nature of this TS.

For the cationic system, the geometries of the rhodium squared-planar complex **17a**, the possible isomers of the oxidative addition products (**20a-*cis*** and **20a-*trans***), as well as

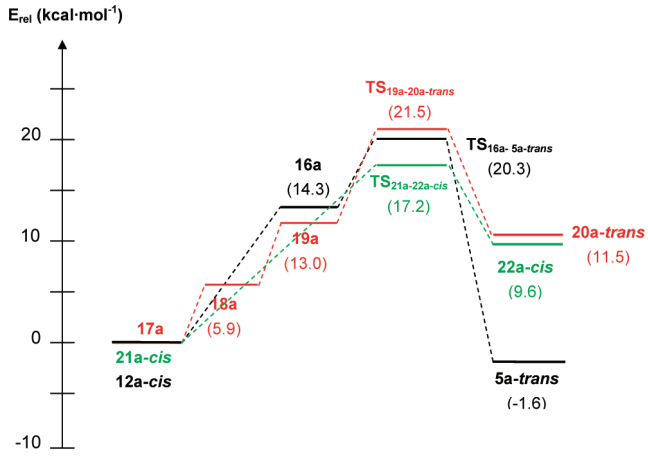

Figure 5. Calculated pathway for the oxidative addition process. Relative energies are given in kcal·mol^{-1} (in parentheses).

the corresponding transition state were determined. First, the results showed that the most favored pathway, although endothermic, corresponds to the formation of **20a-*trans*** (Figure 3). The relative energy of the transition state $\mathbf{TS_{19a\text{-}20a\text{-}trans}}$ was computed to be 21.4 kcal·mol^{-1} above the corresponding reactant **17a**, while the energy of the *cis* product was even higher. Note that the coordination mode of aldimine in **17a** does not allow the reaction to proceed further. So, from the chelating coordination mode **17a**, decoordination and rotation around the C−N bond are needed to enable the C−H bond in close proximity to the metal atom. Indeed, two new intermediates, **18a** and **19a**, that are both less stable than the reactant were characterized along the reaction coordinate.

Furthermore, as the aldimine **3** is in excess under catalytic conditions with respect to the Rh catalyst, the coordination of a second aldimine molecule to the rhodium center could not be discarded during the catalytic process. For this purpose, a pyridine molecule was used to model the aldimine in order to reduce the computational cost. As in the previous cases, reactants **21a**, transition state $\mathbf{TS_{21a\text{-}22a}}$, and the corresponding product **22a** were characterized. In this case, the isomer **21a-*trans*** is slightly more stable than **21a-*cis***, but the energy barrier required to reach the TS by following the *trans* complex (37.1 kcal·mol^{-1}) is much higher than the barrier for the *cis* 18.5 kcal·mol^{-1} (Figure 4). In both cases, the products are less stable than the corresponding reactants.

Figure 5 shows the reaction energy profile for the neutral complex (black line), the cationic (red line), and the cationic with pyridine (green line) complexes. In the neutral pathway, the reaction is initiated by an interaction (**16a**) between the rhodium, carbon, and hydrogen involved in the oxidative addition process. The transition state was found to have an energy of 20.3 kcal·mol^{-1} relative to the starting material. The evolution of this TS affords the complex **5a-*trans***, which is the product of the oxidative addition process. The reaction is exothermic, and thus the formation of this product is favored. For the cationic complex **17a** (red line), the energy barrier is higher than for the neutral system (black line), and the reaction is therefore expected to be slower. Furthermore, for this cationic system, the oxidative addition was found to be endothermic, and the formation of the product is therefore disfavored. Moreover, in the cationic pyridine system **21a**, the energy barrier is lower than in the neutral system. In both cationic complexes, the reaction is endothermic. It is interesting to note that the transition state geometries are very similar in all three cases; the distances and angles did not present significant differences. The angle between the two phosphorus atoms and the metallic center (P−Rh−P) and the carbon−hydrogen (C−H) distance involved in the oxidative addition process were the two parameters that changed the most. Regarding the P−Rh−P angle, in the transition state $\mathbf{TS_{16a\text{-}5a\text{-}trans}}$, it was found to have the widest angle (117.6°); this angle was 90.8 and 95.9° for $\mathbf{TS_{19a\text{-}20a\text{-}trans}}$ and $\mathbf{TS_{21a\text{-}22a\text{-}cis}}$, respectively. Moreover, $\mathbf{TS_{16a\text{-}5a\text{-}trans}}$ showed the longest C−H bond (1.76 Å), while the $\mathbf{TS_{19a\text{-}20a\text{-}trans}}$ and the $\mathbf{TS_{21a\text{-}22a\text{-}cis}}$ showed a C−H distance equal to 1.58 and 1.51 Å, respectively. This analysis shows that the three transition states are very similar and that their structure is close to the corresponding reactant.

These calculations show that, during the oxidative addition, noticeable changes in the angle P−Rh−P are required. For instance, in the neutral system **12a-*cis***, the P−Rh−P angle was 95.1°; in the transition to the intermediate **16a**, this angle was 101.5°. When the TS was achieved, the angle increased to 117.6°. Finally, in the oxidative addition product **5a-*trans***, this value increased again to 163.2°. Such variations indicate that the use of monodentate phosphines is suitable for this process. Furthermore, while the reaction is clearly exothermic only in the case of the neutral system, the energy barriers in the cationic and in the neutral pathway are relatively similar. This indicates that the role of chloride when it is coordinated to the rhodium complex is to increase the stability of the oxidative addition product, enabling the reaction to continue. This is not the case in the cationic complexes since the low stability of the reaction products promotes the back reaction and, therefore, low conversions are obtained.

Study of the Alkene Insertion and Reductive Elimination by in situ NMR. Reactivity of 5-*trans* in the Presence of Styrene. In order to investigate the insertion of the alkene into the hydride **5-*trans***,[26] a 5 mm NMR tube was charged with a solution of **5-*trans*** in toluene-d_8, and 5 equiv of styrene was added under N_2 atmosphere. When ^{1}H and ^{31}P{^{1}H} spectra were recorded at 295 K, only signals corresponding to the reagents were apparent. The temperature was gradually increased up to 373 K, and spectra were recorded at intervals of 10 K. No changes were observed in the ^{31}P{^{1}H} NMR spectra between 295 and 363 K. At 363 K, two new ^{31}P signals were detected at δ 45.5 (d, $J_{Rh,P}$ = 163 Hz) and 52.9 (d, $J_{Rh,P}$ = 198 Hz). The latter resonance was readily assigned to the previously reported dimeric species [Rh(μ-Cl)(PPh$_3$)$_2$]$_2$ (**11**)[29] (Figure 6a). It was concluded that the signal resonating at δ 45.5 and exhibiting a Rh−P coupling corresponded to a newly formed Rh species that contained at least one PPh$_3$ ligand. After a few minutes at this temperature, the signal corresponding to [Rh(μ-Cl)(PPh$_3$)$_2$]$_2$ was not observed, and a new resonance was detected at δ −4.7 (broad singlet), which was readily assigned to free PPh$_3$. The signal at δ 45.5 and that of free PPh$_3$ increased in intensity, while the resonance corresponding to the starting complex **5-*trans*** decreased (Figure 6b).

The identity of the new species formed was investigated using ^{1}H, ^{13}C, COSY, ^{1}H−^{13}C HSQC, and ^{1}H−^{13}C HMBC techniques. The most relevant data are the following: two proton signals at δ 2.75 (dd, J_{HH} = 7 and 14 Hz, 1H) and 3.20 (dd, J_{HH} = 8 and 14 Hz, 1H) were found to correlate with a ^{13}C signal at δ 38.1 exhibiting a singlet multiplicity, indicating the presence of a CH$_2$ unit; one ^{1}H resonance at δ 3.13 (q, J_{HH}= 8 Hz, 1H) was correlated with a doublet ^{13}C signal at δ 52.4 (J_{RhC} = 15.5 Hz), and phase discrimination indicated the presence of a CH unit; HMBC analysis showed that the latter unit was neighboring

(29) Naaktgeboren, A. J.; Nolte, R. J.; Drenth, W. *J. Am. Chem. Soc.* **1980**, *102*, 3350.

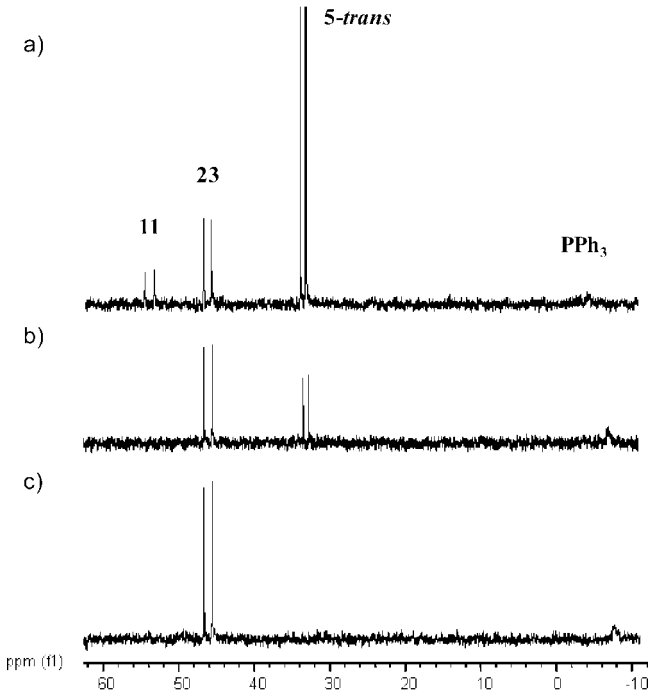

Figure 6. Sequence of $^{31}P\{^1H\}$ spectra of a toluene-d_8 solution containing **5-*trans*** and styrene: (a) at 363 K; (b) at 363 K after a few minutes; (c) at rt after reaction.

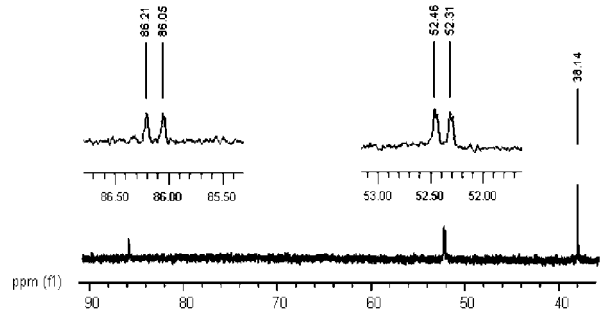

Figure 7. Selected region of the $^{13}C\{^1H\}$ spectrum of **23** at room temperature.

the previously mentioned CH_2 unit and another group containing a quaternary carbon atom that resonated at δ 86.1 as a doublet (J_{RhC} = 15.5 Hz).

The higher chemical shift for the latter resonance (86.1 ppm) indicated the presence of a neighboring heteroatom. Furthermore, the detection of the signals at δ 52.4 and 86.1 as Rh-coupled resonances indicated that the corresponding carbon atoms were bound to the Rh center (Figure 7). It was therefore concluded that a $-CH_2-CH{=}C(R')N-$ unit was contained in the new product and was bound to the Rh center through the C=C double bond in an η^2-manner. The absence of P−C coupling suggested that the vinylic moiety is situated in *cis* position to the phosphine ligand(s). After analysis of the NMR spectra, the product was identified as [RhCl(PPh$_3$)(**24a**)] (**23**, Figure 8). To the best of our knowledge, this species has not been reported. The detection of this species reveals a tautomeric process between the organic products **24** and **24a** (Scheme 5).

When the temperature of the sample was increased to 373 K, the intensity of ^{31}P signals corresponding to the starting complex **5-*trans*** and to the dimeric species [Rh(μ-Cl)(PPh$_3$)$_2$]$_2$ (**11**) rapidly decreased, while those of **23** and free PPh$_3$ increased. After 2 h at this temperature, the only Rh species detected in solution was **23** (Figure 6c).

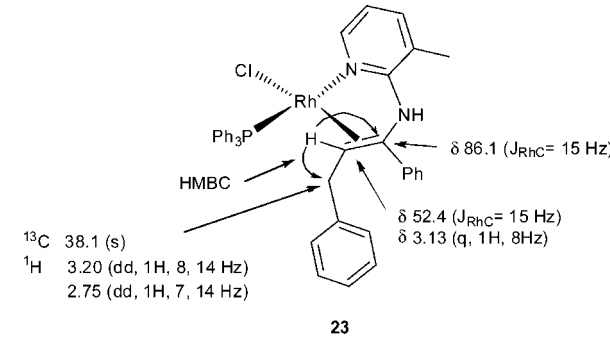

Figure 8. Relevant NMR data for complex **23**.

Scheme 5. Tautomerism of 24

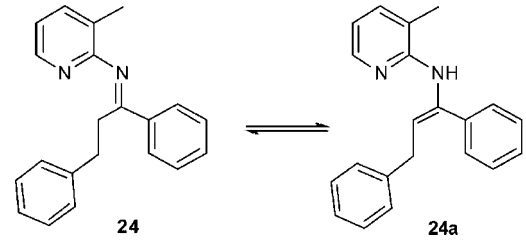

Scheme 6. Reaction of 5-*trans* Styrene in the Presence of Aldimine 3

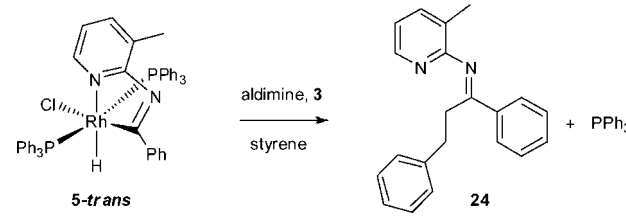

When the temperature of the sample was decreased to 295 K and the sample was taken out of the NMR spectrometer, red crystals were observed at the bottom of the NMR tube. X-ray analysis of these crystals confirmed the identity of the complex [Rh(μ-Cl)(PPh$_3$)$_2$]$_2$.

Reaction of 5-*trans* in the Presence of Styrene and Aldimine 3. In order to investigate the effect of the presence of substrate excess, the reaction was repeated in the presence of 5 equiv of aldimine **3**. The temperature was gradually increased up to 373 K, and the reaction was monitored by ^1H and ^{31}P NMR spectroscopy. As previously observed, the presence of free PPh$_3$ ligand in solution was observed at 353 K. Even at higher temperatures, however, no new ^{31}P signals were detected. At 363 and 373 K, the signal corresponding to the starting complex **5-*trans*** decreased in intensity, while that corresponding to free PPh$_3$ proportionally increased. Even after a few hours at 373 K, however, the signal corresponding to **5-*trans*** was still visible. In the ^1H spectra, the only new signals detected were assigned to the organic product **24** formed by the catalytic reaction (Scheme 6).

The presence of **11** in Figure 6a in its further disappearance (Figure 6b) indicates that **23** is probably formed through isomerization of **14** induced by **11** and coordination of the tautomeric form **14a**. On the basis of these results, the catalytic cycle described in Scheme 7 is proposed.

Formation of Cationic Rhodium Hydride Complex from 5-*trans* and Study of the Reactivity with Styrene. Formation of Cationic Rhodium Hydride Complexes. In the study of the oxidative addition of **3** to cationic rhodium complexes, no hydride species could be detected (Scheme 4);

Scheme 7. Proposed Catalytic Cycle for the Hydroiminoacylation of Styrene Catalyzed by Neutral Rh Systems

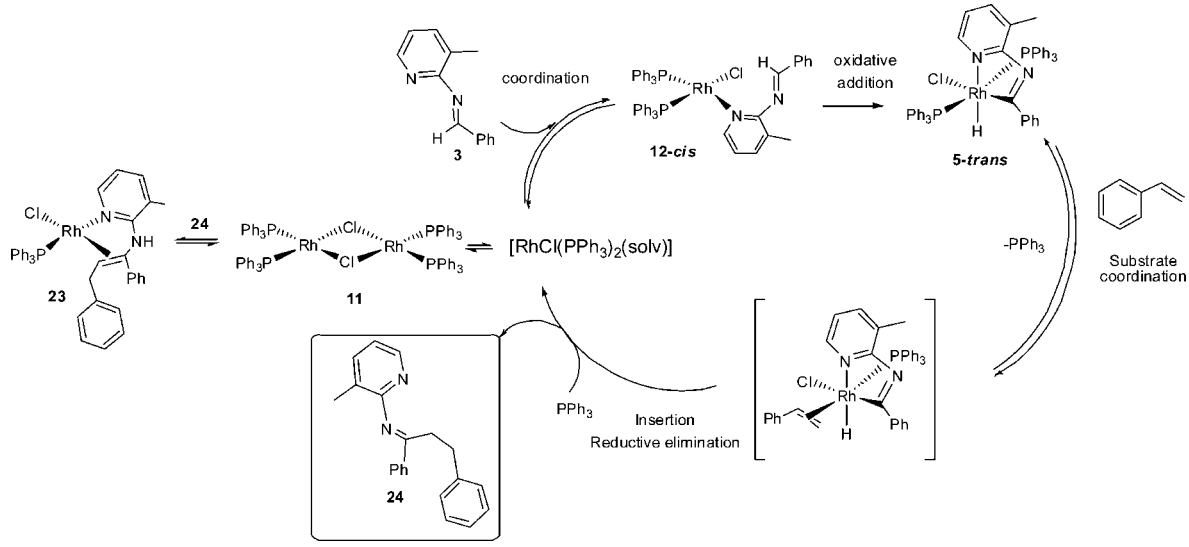

however, the very low conversions obtained with these systems indicate that such species could be formed although to a small extent.

It was therefore decided to form cationic rhodium hydride complexes in situ and probe their reactivity toward styrene. With this aim, **5-*trans*** was dissolved in CD_2Cl_2, cooled to 193 K, and 1 equiv of $AgBF_4$ was added. The tube was quickly transferred into the NMR spectrometer that had been precooled to 193 K, and ^1H and $^{31}P\{^1H\}$ spectra were recorded; only signals corresponding to the starting complex **5-*trans*** were observed (Figure 9a).

The tube was then briefly taken out of the spectrometer, shaken at room temperature for a short time, and reinserted into the NMR probe. In the ^1H spectrum recorded at 193 K, a hydride signal was then detected at δ −10.9 (dt, J_{RhH} = 16 Hz, J_{PH}= 9 Hz). In the corresponding $^{31}P\{^1H\}$ spectrum, a new signal was detected at δ 36.8 (d, J_{RhP}= 114 Hz). The tube was warmed in the same manner a few times, and it was observed that the new signals increased in intensity, while the signals for **5-*trans*** decreased in the same proportion (Figure 9b). The new hydride product was found to exhibit spectral features similar to those of **5-*trans***, indicating small structural differences with **5-*trans***.

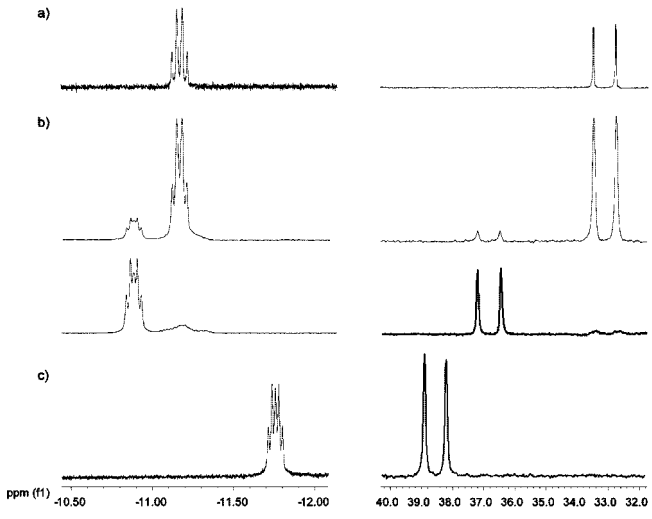

Figure 9. (a) ^1H and $^{31}P\{^1H\}$ spectra of **5-*trans*** in CD_2Cl_2. (b) ^1H and $^{31}P\{^1H\}$ of **20-*trans*** formation in CD_2Cl_2. (c) ^1H and $^{31}P\{^1H\}$ spectra of cationic complex with pyridine, **22-*trans***, in CD_2Cl_2.

Scheme 8. Formation of Cationic Hydride Rhodium Complexes 20-*trans*, 22-*trans*, and 25

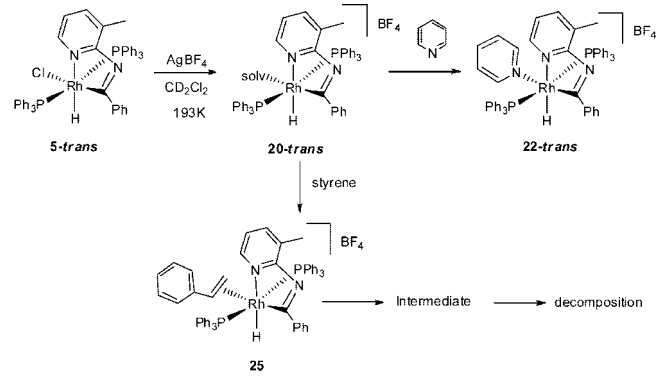

The multiplicity of the hydride signal indicated that this species contained two equivalent PPh_3 ligands. The new complex was identified as **20-*trans*** (Scheme 8) with one solvent molecule coordinated to the rhodium center.

When the temperature of the sample was slowly increased to room temperature, the broadening of the NMR signals for the new complex was observed, and at 293 K, the presence of bulk rhodium metal in the sample was evident, indicating the decomposition of the complex. The instability of this species upon warming is in contrast with the report of Suggs, which described an analogue Rh hydride complex containing a chelating acyl−quinonoline moiety as an indefinitely stable species at room temperature.[7]

In order to probe the presence of a solvent molecule in this complex, the reaction was repeated, and 5 equiv of pyridine was added to the solution at low temperature, and new ^1H and $^{31}P\{^1H\}$ spectra were recorded. In the $^{31}P\{^1H\}$ spectrum, a new doublet signal was detected at δ 38.5 (J_{RhP} = 114 Hz). In the ^1H spectrum, a new hydride signal was evident as a doublet of triplets at δ −11.8 (J_{RhH} = 16 Hz, J_{PH} = 9 Hz) (Figure 9c). A set of new aromatic peaks was also detected. When the temperature was slowly increased, some of the aromatic resonances were observed to coalesce; this effect was attributed to the rotation of a pyridine ligand. At room temperature, the signals corresponding to the new species were found to slightly broaden, but the complex was found to be stable for a few hours under these conditions. This new species was fully characterized by NMR spectroscopy and identified as **22-*trans*** (Scheme 8).

It is noteworthy that species **22-*trans*** corresponds to the calculated species **22a-*trans***, which was shown to be more stable than the *cis* isomer by DFT calculations. The high energy of $\mathbf{TS_{21a\text{-}22a\text{-}}trans}$ indicated that the *cis* pathway is preferred and that further isomerization proceeds after the CH activation process.

Reaction of [RhH{benzylidene-(3-methylpyridine-2-yl)amine}(PPh_3)$_2$(solv)][BF_4] (20-*trans*) in the Presence of Styrene. In order to investigate the reactivity of **20-*trans*** in the presence of styrene, an NMR tube was charged with **5-*trans*** in CD_2Cl_2 and reacted with $AgBF_4$ in situ. The formation of **20-*trans*** was monitored by ^{31}P NMR spectroscopy. Three equivalents of styrene was then added at 193 K, and the tube was transferred into the precooled spectrometer at 193 K. The temperature of the sample was then gradually increased, and the reaction was monitored by ^{1}H and ^{31}P NMR. No new products were detected up to 233 K. At 243 K, a broad ^{31}P signal was detected at δ 36.75 (d, J_{RhP} = 110 Hz). In the corresponding ^{1}H spectrum, a new broad hydride signal was detected at δ −10.24. These signals were assigned to the alkene complex **25**. Upon warming, a new hydride was detected at δ −10.66. Two new doublet signals were also detected in the ^{31}P{^{1}H} spectrum at δ 18.6 (d, J_{RhP} = 75 Hz) and 14.1 (d, J_{RhP} = 75 Hz). At 295 K, the hydride signal resonating at δ −10.24 rapidly decreased, while the intensity of the signal at δ −10.66 increased. After a few minutes, the signals corresponding to **25** (Scheme 8) could not be detected. Upon increasing the temperature, the ^{31}P signals resonating at δ 18.6 and 14.1 were found to broaden and finally to coalesce at δ 16.5 at 295 K. At this temperature, however, all the signals were found to broaden rapidly, and rhodium metal was observed in the NMR tube, indicating that the species present in solution were decomposing. The identity of the hydride species could not be determined; however, the presence of a hydride ligand indicated that the insertion of styrene into the Rh−H bond of **25** had not occurred. After a few hours at 295 K, the hydride signal was not observed, although the ^{31}P signal resonating at δ 16.5 was still detected, indicating that this signal was not correlated with the previously mentioned hydride species. No evidence for the formation of a new Rh species or the organic catalytic product was obtained when a ^{13}C{^{1}H} spectrum was acquired at this temperature. It was therefore concluded that the insertion of styrene into the Rh−H bond of the cationic system is a slow process, in contrast to the neutral system, for which this step is rapid and yields the intermediate **20-*trans***.

Conclusion

Both cationic and neutral rhodium catalyst precursors were studied in the hydroiminoacylation of alkenes. Catalytic runs revealed that cationic catalysts were poorly active, while the neutral catalyst is active under similar conditions. A study by in situ NMR and DFT calculations allowed us to explain these differences based on the following facts: (a) The neutral rhodium complex [RhCl(PPh_3)$_3$] reacts at low temperature with aldimine **3** to give the oxidative addition product **5-*trans***, while the cationic rhodium complex [Rh(NBD)(PPh_3)$_2$]BF_4 (**13**) does not react with aldimine **3** to give any stable oxidative addition products even at higher temperature. (b) The oxidative addition step is an exothermic process for neutral systems, whereas it is endothermic for cationic systems. (c) The calculated energy barriers in the cationic and in the neutral pathways are relatively similar. (d) The coordination and insertion of the alkene is very rapid for the neutral system, while in the cationic system the coordination is slow and the insertion was not detected. (e) The reductive elimination product was fully characterized for the neutral system as a complex containing the coordinated organic product in its enamine tautomeric form (**23**), while for the cationic system, no resulting complex neither hydroiminoacylation product could be detected.

In summary, this study indicates that the role of the chloride ligand is to increase the stability of the oxidative addition product. In the case of the cationic complexes, the lower stability of the oxidative addition product was evidenced. The failure of the cationic catalysts is likely due to a higher energetic barrier for one of the following steps of the catalytic cycle.

Experimental Section

General Procedures. All of the starting materials, reagents, MK-10, and phosphines used were purchased and used without further purification, except the aldehydes, which were distilled prior to use. The catalytic reactions were monitored by GC on a Hewlett-Packard 5890A. Conversion was measured using a HP-5 column (25 m × 0.2 mm ∅). The oven temperature was set to 80 °C for 0.5 min and then increased 10 °C/min to 280 °C. All complexes were synthesized using standard Schlenk techniques under nitrogen atmosphere. Toluene and THF were distilled over sodium/benzophenone, and dichloromethane was dried over P_2O_5. All solvents were deoxygenated before use. RhCl(PPh_3)$_3$ was purchased from Strem Chemicals and $AgBF_4$ from Sigma-Aldrich; both were used without further purification. The reagents used for the synthesis of **3** were purchased from Sigma-Aldrich. Complex **5-*trans*** was prepared according to literature methods.[26] All other reagents were used as received from commercial suppliers. All the deuterated solvents of grade 99.8%D packed in sealed ampules were purchased from Euriso-top. ^{1}H, ^{13}C{^{1}H}, and ^{31}P{^{1}H} spectra were recorded on a Varian Mercury 400 spectrometer (400.14, 100.63, and 161.98 MHz, respectively). Chemical shifts were referenced to either TMS as an internal standard (^{1}H and ^{13}C) or 85% H_3PO_4 as an external standard (^{31}P). Gas chromatography was performed in a Hewlett-Packard 5890A apparatus (T = 80 °C for 0.5 min up to 280 °C; rate = 10 °C/min).

Computational Methods: All DFT calculations were performed using the Amsterdam density functional (ADF2004.01) program developed by Baerends et al.[30−32] Local VWN[33] exchange-correlation potential with nonlocal Becke's exchange correction[34] and Perdew's correlation correction[35] (BP86) were used. Relativistic corrections were introduced by scalar-relativistic zero order regular approximation (ZORA).[36−38] A triple-ζ plus polarization basis set was used on all atoms. For non-hydrogen atoms, a relativistic frozen-core potential was used, including 4d for rhodium, 2p for phosphorus and chlorine, 3p for iodine, and 1s for carbon and nitrogen. The Slater basis sets were extracted from the ADF library. Transition states were fully characterized by means of vibrational frequencies analysis. Also, a pseudo-IRC procedure was followed in order to connect the TS to the corresponding reactant and product, which consisted of adding or subtracting the imaginary normal mode vector to the coordinates of the transition state geometry, and subsequent energy minimization.

(30) Baerends, E. J.; Ellis, D. E.; Ros, P. *Chem. Phys.* **1973**, *2*, 41.
(31) te Velde, G.; Bickelhaupt, F. M.; van Gisbergen, S.; Guerra, C. F.; Baerends, E.; Snijders, J.; Ziegler, T. *J. Comput. Chem.* **2001**, *22*, 931.
(32) Guerra, C. F.; Snijders, J.; te Velde, G.; Baerends, E. *Theor. Chem. Acc.* **1998**, *99*, 391.
(33) Vosko, S. H.; Wilk, L.; Nusair, M *Can. J. Phys.* **1980**, *58*, 1200.
(34) Becke, A. *Phys. Rev. A* **1988**, *38*, 3098.
(35) (a) Perdew, J. P. *Phys. Rev. B* **1986**, *34*, 7406. (b) Perdew, J. P. *Phys. Rev. B* **1986**, *33*, 8822.
(36) van Lenthe, E.; Baerends, E.; Snijders, J. *J. Chem. Phys.* **1993**, *99*, 4597.
(37) van Lenthe, E.; Baerends, E.; Snijders, J. *J. Chem. Phys.* **1994**, *101*, 9783.
(38) van Lenthe, E.; Ehlers, A.; Baerends, E.; Snijders, J. *J. Chem. Phys.* **1999**, *110*, 8943.

General Procedure for the Intramolecular Hydroacylation of Alkenes Using Cationic Systems and Chlorine Source: A mixture of benzaldehyde (2.5 mmol), 2-amino-3-picoline (0.8 mmol), 1-hexene (12.5 mmol), MK-10 (80 mg), [Rh(cod)L_2] and PR_3 (0.05 mmol), and $BnMe_3NCl$ (0.05 mmol) or alternatively $RhCl(PPh_3)_3$ (0.05 mmol) in 2 mL of toluene was heated to 110 °C for 2 h. The resulting mixture was filtered and analyzed by GC.

Typical Procedure for the Preparation of NMR Samples: Typically, a 5 mm NMR tube fitted with a Young's valve was charged with ca. 15 mg of rhodium complex and dissolved in the appropriate deuterated solvent. Addition of the reagent(s) was completed under inert atmosphere and low temperature when required. The sample was then transferred into the NMR spectrometer, which was previously set to the appropriate temperature.

Heptanophenone (10): ^{1}H NMR ($CDCl_3$, 400 MHz) δ = 7.95 (dd, J = 5.2 Hz, 1H, H-6 Py), 7.55−7.95 (m, 2H, Ph), 7.35 (dd, J = 5.2 Hz, 1H, H-4 Py), 6.90−7.10 (m, 3H, Ph), 6.66−6.76 (m, 1H, H-5 Py), 2.60 (t, J = 7.9 Hz, 2H, hexyl), 2.17 (s, 3H, CH_3 Py), 1.10−1.60 (m, 8H, hexyl), 0.80 (t, J = 6.8 Hz, 3H, CH_3 hexyl); ^{13}C NMR ($CDCl_3$, 100.6 MHz) δ = 171.3 (−C═N), 161.8 (C-2 Py), 148.3 (C-4 Py), 146.3 (C-6 Py), 138.7−120.3 (Ph), 119.4 (C-5 Py), 117.9 (C-3 Py), 31.4, 30.1, 29.8, 21.1 (C-hexyl), 18.8 (CH_3 Py), 13.8 (CH_3 hexyl), 2.3 (C-hexyl).

Preparation of 2-Benzylidene-3-methylpyridine (3): The synthesis of this compound was completed according to reported literature methods.[39] A solution of 4.83 g (44.6 mmol) of 2-amino-3-picoline (**2**) in 20 mL of THF was prepared, and 5 mL (49.2 mmol) of benzaldehyde (**1**) was added in the presence of molecular sieve (4 Å). The reaction mixture was refluxed for 12 h and then cooled to rt. The molecular sieve was removed by filtration. The solvent was evaporated in vacuo, and the resulting oily residue was distillated under vacuum using a Buchi GKR-51 Kugelrohr oven; a yellow liquid was isolated (yield = 7.88 g, 90%). Although this procedure was previously reported, no precise NMR data were found to be available. Here, we list the ^{1}H and ^{13}C data for **3**: ^{1}H NMR ($CDCl_3$, 400 MHz) δ = 9.1 (s, 1H, HC═N), 8.3 (dd, J = 1.6 and 4.8 Hz, 1H, Py), 8.00 (dd, J = 2.4 and 7.2 Hz, 2H, Ph), 7.54 (d, 1H, J = 7.6 Hz, Py), 7.48 (m, 3H, Ph), 7.07 (dd, 1H, J = 4.8 and 7.2 Hz), 2.46 (s, 3H, CH_3); ^{13}C NMR ($CDCl_3$, 100.6 MHz) δ = 161.3 (−C═N), 159.2, 145.9, 136.6, 131.5, 129.6, 129.2, 128.9, 128.5, 127.4, 121.7, 17.5.

Preparation of [RhHCl{(2-benzylidene)-3-methylpyridine}-(PPh_3)$_2$] (5-*trans*): A solution of Wilkinson's catalyst $RhCl(PPh_3)_3$ (0.5 g, 0.54 mmol) and 2-benzylidene-3-methylpyridine **2** (0.1 g, 0.51 mmol) in ca. 35 mL of THF was refluxed for 3 h. Half of the solvent was removed in vacuo, and precipitation of the product was achieved by addition of cold *n*-hexane. After filtration, the product was isolated as a pale yellow solid (0.35 g, 80% yield): ^{1}H NMR ($CDCl_3$, 400 MHz) δ = 8.39 (d, 1H, J = 5.6 Hz, Py), 7.65 (d, 2H, J = 7.2 Hz, Ph), 7.43 (m, 12H, PPh_3), 7.28 (d, 1H, J = 7.6 Hz, Py), 7.13 (m, 18H, Ph), 6.87 (t, 1H, J = 7.2 Hz, PPh_3), 6.68 (dd, 2H, J = 7.2 and 8.6 Hz, PPh_3), 6.52 (dd, J = 5.6 and 7.6 Hz, Py), 2.5 (s, 3H, CH_3), −11.2 (q, J_{RhH} = J_{PH} = 13 Hz); ^{13}C NMR (toluene-d_8, 100.6 MHz) δ = 230.5 (dt, J_{RhC} = 32.6 Hz, J_{PC} = 7.5 Hz), 184.9−118.9 (Ar), 19.2 (CH_3); ^{31}P NMR ($CDCl_3$, 161.9 MHz) δ = 33.1 (d, J_{RhP} = 116.6 Hz).

[RhCl{(2-benzylidene)-3-methylpyridine}(PPh_3)$_2$] (12-*cis*): ^{1}H NMR (CD_2Cl_2, 400 MHz, 253 K) δ = 9.1 (s, 1H, N═CHPh), 9.0 (dd, 1H, J = 5 and 1.8 Hz, Py), 8.90−6.8 (m, 37H, arom), 2.45 (s, 3H, CH_3); ^{31}P NMR ($CDCl_3$, 161.9 MHz, 253 K) δ = 54 (dd, J_{RhP} = 196 Hz, J_{PP} = 47 Hz), 50 (dd, J_{RhP} = 170 Hz, J_{PP} = 47 Hz).

[RhCl{(1,3-diphenylpropenyl)-(3-methylpyridin-2-yl)amine}(PPh_3)] (23): ^{1}H NMR (toluene-d_8, 400 MHz) δ = 9.19 (d, 1H, J = 5.6 Hz, Py), 7.54−6.20 (m, 27H, arom), 3.20 (dd, 1H, J = 14 and 8 Hz), 3.13 (q, 1H, J = 8 Hz), 2.75 (dd, 1H, J = 14 and 7 Hz), 1.30 (s, 3H, CH_3); ^{13}C NMR (toluene-d_8, 100.6 MHz) δ = 158.9−113.3 (Ar), 86.1 (d, J_{RhC} = 15.5 Hz), 52.4 (dd, J_{RhC} = 15.5 Hz, J_{PC} = 2.3 Hz), 38.1, 16.5 (CH_3); ^{31}P NMR (toluene-d_8, 161.9 MHz) δ = 45.5 (d, J_{RhP} = 163 Hz).

[RhH{(2-benzylidene)-3-methylpyridine}(PPh_3)$_2$(solv)]BF_4 (20-*trans*): ^{1}H NMR (CD_2Cl_2, 400 MHz, 233 K) δ = 8.23 (d, 1H, J = 4.4 Hz, Py), 7.61 (d, 2H, J = 7.6 Hz, Ph), 7.33−7.20 (m, 31H, arom), 7.1−6.78 (m, 4H, Py and Ph), 2.23 (s, 3H, CH_3), −10.86 (overlapping d of t, 1H, J_{RhH} = 16 Hz, J_{PH} = 9 Hz); ^{31}P NMR ($CDCl_3$, 161.9 MHz, 233 K) δ = 36.8 (d, J_{RhP} = 118 Hz).

[RhH{(2-benzylidene)-3-methylpyridine}(PPh_3)$_2$(pyridine)]BF_4 (22-*trans*): ^{1}H NMR (CD_2Cl_2, 400 MHz, 298 K) δ = 8.57 (br s, free py), 8.22 (d, 1H, J = 5.2 Hz), 8.15 (br s, 1H, py), 7.81 (dd, 2H, J = 8 and 1.2 Hz), 7.7−7.1 (m, 42H), 6.94 (t, 2H, J = 8 Hz), 2.14 (s, CH_3), −11.8 (overlapping d of t, 1H, J_{RhH} = 16 Hz, J_{P-H} = 9 Hz); ^{31}P NMR (CD_2Cl_2, 161.9 MHz, 298 K) δ = 38.5 (d, J_{RhP} = 114 Hz).

Acknowledgment. The authors acknowledge the financial support of MICINN (CTQ2008-001569) (CTQ2008-06549-C02-02), and Consolider Ingenio 2010, CSD2006-0003 (Ministerio de Educación, Spain), and the ICIQ Foundation. We thank Servei de Recursos Científics (URV) for technical assistance. Fellowships to P.M. and Juan de la Cierva fellowship to C.G. from MEC are also acknowledged. We also thank Prof. Piet W.N.M. van Leeuwen for the critical reading of the manuscript.

Supporting Information Available: Tables giving pictures, energies, and Cartesian coordinates for all calculated structures, and comparison of X-ray determined and calculated selected parameters for **5-*trans*-I**. This material is available free of charge via the Internet at http://pubs.acs.org.

OM800827R

(39) Chul-Ho, J. *Bull. Korean Chem. Soc* **1990**, *11*, 187.